Dyes and Pigments 90 (2011) 284–289

Contents lists available at ScienceDirect

Dyes and Pigments

journal homepage: www.elsevier.com/locate/dyepig

Concentration and pH-modulated dual fluorescence in self-assembled nanoparticles of phototautomerizable biopolymeric amphiphile

Chang-Keun Lim [a], Jangwon Seo [b], Sehoon Kim [a,*], Ick Chan Kwon [a], Cheol-Hee Ahn [c,***], Soo Young Park [b,**]

[a] Biomedical Science Center, Korea Institute of Science and Technology, 39-1 Hawolgok-dong, Seongbuk-gu, Seoul 136-791, Republic of Korea
[b] Center for Supramolecular Optoelectronic Materials, WCU Program for Hybrid Materials, Seoul National University, 599 Gwanak-ro, Gwanak-gu, Seoul 151-744, Republic of Korea
[c] Department of Materials Science & Engineering, Seoul National University, 599 Gwanak-ro, Gwanak-gu, Seoul 151-744, Republic of Korea

ARTICLE INFO

Article history:
Received 27 October 2010
Received in revised form
20 December 2010
Accepted 26 December 2010
Available online 7 January 2011

Keywords:
Excited-state intramolecular proton transfer (ESIPT)
Ratiometric fluorescence sensor
Fluorescent nanoparticle
pH sensor
Self-assembly
Biopolymeric conjugate

ABSTRACT

A dual-emissive biopolymeric amphiphile (GC–HBO) has been prepared by densely conjugating hydrophilic glycol chitosan (GC) with a phototautomerizable hydrophobic dye (a derivative of 2-(2′-hydroxyphenyl) benzoxazole, HBO) showing excited-state intramolecular proton transfer (ESIPT). Ratiometric modulation of phototautomeric (enol–keto) dual emission, governed by the chromophoric aggregation state, was studied with a low-molecular-weight model compound (GA–HBO) and was well correlated with the nanoparticle-forming behavior of GC–HBO via amphiphilic self-assembly in water. It has been found that the promoted chromophoric aggregation at higher concentration or at basic-to-neutral pH assists the nanostructure formation to generate predominant keto emission while the enol emission is intensified at lower concentration or with decreasing pH by disintegration of self-assembled structure. The assembly-related advantageous potential of GC–HBO for probing self-concentration and surrounding pH has been demonstrated with the ratiometric determination of critical particulation concentration (0.04 kg m^{-3}) and near-physiological pH sensitivity ($pK_a \sim 5.1$).

1. Introduction

Luminescence-based technologies have led to great leaps in biological, medical, environmental and material sciences. Recently, molecules capable of fluorescence switching are gaining great interest for their potential utility from typical polarity–viscosity probes to more advanced applications including biosensors, logic gates, and optical recordings [1–5]. Aggregation-triggered fluorescence modulation is a more recent and special example [6–11], which offers a novel pathway to fluorescence probing of molecular aggregation-related phenomena.

Aggregation of amphiphiles is a key way of molecular organization in biological systems and often employed to develop biomimetic supramolecular materials. Biopolymeric amphiphiles with an appropriate hydrophilic/hydrophobic balance are an emerging class of biohybrid nanomaterials that form self-assembled nanoparticles in aqueous milieu with the interfacial-free energy-minimized structure comprising a hydrophilic shell and hydrophobic multicores. Hydrophobically modified glycol chitosan is among the representative examples that hold considerable potential as drug carriers and bioimaging agents due to high biocompatibility and high tumor targeting efficiency [11–15]. Basic studies on the nanoparticulate characteristics of biopolymeric amphiphiles are a research subject of great importance to understand their advantageous behaviors in a complex in vivo environment [12,14].

In this study, we applied the aggregation-induced fluorescence modulation to probing the concentration and pH-dependant assembly of biopolymeric amphiphiles in aqueous phase. To this end, we designed a novel dye-concentrated biohybrid that can self-probe its own molecular aggregation state with ratiometric fluorescence modulation. As depicted in Fig. 1, the designed biohybrid (GC–HBO) is composed of water-soluble glycol chitosan (GC) and a derivative of 2-(2′-hydroxyphenyl)benzoxazole (HBO) as a densely conjugated hydrophobic pendant. The HBO unit is a well-known chromophore exhibiting enol-to-keto phototautomerization via the excited-state intramolecular proton transfer (ESIPT) reaction. Its dual fluorescence from each phototautomer is independently responsive

* Corresponding author. Tel.: +82 2 958 5924; fax: +82 2 958 5909.
** Corresponding author. Tel.: +82 2 880 8347; fax: +82 2 886 8331.
*** Corresponding author. Tel.: +82 2 883 8197; fax: +82 2 880 5791.
E-mail addresses: sehoonkim@kist.re.kr (S. Kim), chahn@snu.ac.kr (C.-H. Ahn), parksy@snu.ac.kr (S.Y. Park).

0143-7208/$ – see front matter © 2011 Elsevier Ltd. All rights reserved.
doi:10.1016/j.dyepig.2010.12.014

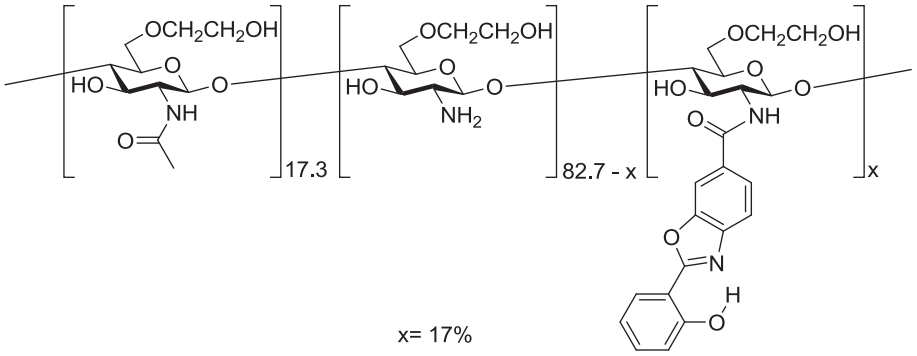

Fig. 1. Phototautomerizable Amphiphilic Glycol Chitosan (GC–HBO).

to environmental parameters (medium polarity–viscosity, pH, and temperature, etc.) [16–19]. In particular, it has recently been reported that in some ESIPT molecules, the weak proton-transferred keto emission in solution is greatly enhanced over the enol emission by solidification [19–22], allowing for highly reliable ratiometric optical probing of molecular aggregation. Ratiometric fluorescence method offers advantages of increased dynamic range of detection and built-in correction for environmental effects by eliminating data distortions caused by instrumental instability, photobleaching, and probe concentration [23]. Here are reported the synthesis of GC–HBO as a polymeric model biohybrid and its concentration and pH dependent assembly behavior, along with a low-molecular-weight model study on the ratiometric fluorescing characteristics of nanoaggregated ESIPT system.

2. Experimental section

Chemical reagents were purchased from Aldrich and used as received. ^{1}H NMR measurements were recorded on an Avance DPX-300 (300 MHz, Bruker, Germany) in $CDCl_3$ and DMSO-d_6 solution. UV–visible absorption and fluorescence spectra were measured on an 8453 UV–Visible spectrophotometer (Agilent Technology, USA) and an F-7000 fluorescence spectrophotometer (Hitachi, Japan), respectively. Transmission electron microscopic (TEM) image of negatively stained particles (with 2 wt.% uranyl acetate) was obtained with a CM30 electron microscope (FEI/Philips) operated at 200 kV. Hydrodynamic size distribution of nanoparticles was determined by dynamic light scattering (DLS) method with a particle sizer (90Plus, Brookhaven Instruments Corporation). The pH-dependence measurements were performed in phosphate buffer saline (PBS, pH 4.0–9.0). Ratios of fluorescence intensities (R) at 510 and 420 nm as a function of pH were theoretically fitted to extract the pKa value by using the following equation:

$$R = \frac{I_{510}}{I_{420}} = \frac{F_{\mathrm{pH4.0}}(510)10^{-\mathrm{pH}} + F_{\mathrm{pH8.0}}(510)10^{-\mathrm{p}Ka}}{F_{\mathrm{pH4.0}}(420)10^{-\mathrm{pH}} + F_{\mathrm{pH8.0}}(420)10^{-\mathrm{p}Ka}} \quad (1)$$

where $F_{\mathrm{pH\ 4.0}}(\lambda)$ and $F_{\mathrm{pH\ 8.0}}(\lambda)$ designate fluorescence intensities of the endpoint species (at pH 4.0 and 8.0) at the considered wavelength (λ) [24].

2.1. Synthesis of 2-(2-hydroxyphenyl)benzo[d]oxazole-6-carboxylic acid (HBO-COOH)

A mixture of 4-amino-3-hydroxybenzoic acid (2 g, 13 mmol) and salicylaldehyde (1.6 g, 13 mmol) in acetic acid (120 cm^3) was stirred for 1 h at room temperature, and then lead acetate (5.8 g, 13 mmol) was added to the mixture. After 1 h stirring at room temperature, the mixture was stirred for 24 h at 150 °C. 350 cm^3 of water was added to the mixture and sodium hydroxide was added slowly to obtain pH 5. The filtered solid was dried and recrystallized from ethyl acetate to give HBO-COOH (0.45 g, 14%). ^{1}H NMR (DMSO-d_6, ppm) 11.04 (s, 1H), 8.32 (s, 1H), 8.06 (d, 2H, J = 8.1 Hz), 7.93 (d, 1H, J = 8.1 Hz), 7.58 (t, 1H, J = 7.5 Hz), 7.16 (d, 1H, J = 8.3 Hz), 7.12 (t, 1H, J = 7.5 Hz).

2.2. Preparation of GC–HBO

Glycol chitosan (GC, MW = 250 kDa; degree of deacetylation = 82.7%; Sigma) (0.025 g, 0.122 mmol (unit)) was dissolved in 2 cm^3 of distilled water with sonication and a DMSO (10 cm^3) solution containing HBO-COOH (0.0125 g, 0.049 mmol), 1-ethyl-3-(3-dimethylaminopropyl) carbodiimide hydrochloride (EDC) (0.014 g, 0.074 mmol) and *N*-hydroxysuccinimide (NHS) (0.0085 g, 0.074 mmol) was added. Then the reaction mixture was stirred at ambient temperature for 24 h. To quantify the substitution ratio, the reaction mixture (0.1 cm^3) was mixed with THF (0.9 cm^3) and centrifuged, to settle down precipitates of the GC–HBO conjugate. The substitution ratio was indirectly determined as 17% through the measurement of the unreacted free HBO-COOH concentration in the supernatant by UV absorbance-based quantification. For further experiments, the remaining reaction mixture was subjected to the successive dialysis against DMSO (48 h) and water (48 h) using a Cellu·Sep membrane (Membrane Filtration Products, Inc., molecular cutoff = 50 kDa). The resulting dispersion of GC–HBO was freeze-dried for characterization and imaging experiments.

2.3. Synthesis of 2-(2-hydroxyphenyl)-N-((2R,3S,4S,5R)-2,4,5-trihydroxy-6-(hydroxymethyl)tetrahydro-2H-pyran-3-yl)benzo[d]oxazole-6-carboxamide (GA–HBO)

D-(+)-Glucosamine hydrochloride (0.084 g, 0.39 mmol, Sigma) was dissolved in 1 cm^3 of distilled water with sonication and a DMSO (5 cm^3) solution containing HBO-COOH (0.1 g, 0.39 mmol), 1-ethyl-3-(3-dimethylaminopropyl) carbodiimide hydrochloride (EDC) (0.112 g, 0.59 mmol) and *N*-hydroxysuccinimide (NHS) (0.068 g, 0.59 mmol) was added. After reaction for 24 h at room temperature, the mixture was diluted with brine and the product was extracted three times with ethyl acetate. The dried product was recrystallized from ethyl acetate to give GA–HBO (0.034 g, 21%). ^{1}H NMR (300 MHz, $CDCl_3$:DMSO-d_6 = 1:1), δ (ppm): 11.00 (s, 1H), 8.54 (s, 1H), 8.28 (d, 2H, J = 8.1 Hz), 8.06 (d, 1H, J = 8.1 Hz), 7.58 (t, 1H, J = 7.5 Hz), 7.16 (d, 1H, J = 8.3 Hz), 7.13 (t, 1H, J = 7.5 Hz), 3.31 (s, 4H), 2.93 (s, 3H), 2.87 (s, 1H), 2.60 (s, 3H). ^{13}C NMR (75 MHz, $CDCl_3$), δ (ppm): 169.82, 166.89, 162.08, 160.03, 149.40, 146.26, 135.55, 128.62, 128.31, 122.52, 120.61, 120.07, 118.44, 113.98, 110.35, 29.25,

28.91. MS (MALDI): calcd for $C_{20}H_{20}N_2O_8$, $m/z = 416.38$; found, $m/z = 413.80$.

2.4. Nanoparticle formation of GC–HBO and GA–HBO

Self-assembled nanoparticles of GC–HBO were prepared by redispersion of the freeze-dried sample in water at 1 mg cm^{-3} under probe sonication at 90 W for 2 min (Sigma Ultrasonic Processor, GEX-600). GA–HBO nanoparticles were prepared by adding a solution (0.3 cm^3, 1×10^{-4} M in THF) to the mixed solution of THF/water with varying water fraction (2.7 cm^3/0 cm^3, 2.1 cm^3/0.6 cm^3, 1.5 cm^3/1.2 cm^3, 0.9 cm^3/1.8 cm^3, 0.3 cm^3/2.4 cm^3 and 0 cm^3/2.7 cm^3) under bath sonication. The pure water suspension was obtained by solvent evaporation of GA–HBO solution (0.3 cm^3, 1×10^{-4} M in THF) and redispersion of the dried sample in water (3 cm^3) under probe sonication.

3. Results and discussion

Synthetic routes of phototautomerizable bio-amphiphiles are described in Scheme 1. ESIPT-exhibiting pendant (HBO-COOH) was obtained by one-pot benzoxazole synthesis comprising in situ Schiff base formation and oxidative ring closure in the presence of lead (IV) acetate [25]. GC–HBO was prepared by amidation between free amines of GC and HBO-COOH (40 mol% fed with respect to the GC monomeric units) in DMSO/water, by using 1-ethyl-3-(3-dimethylaminopropyl)carbodiimide hydrochloride (EDC) and *N*-hydroxysuccinimide (NHS) as coupling agents. The purification was conducted by successive dialysis against DMSO and excess pure water. The mild reaction at ambient temperature for 24 h afforded a biohybrid polymer with 17 mol% HBO substitution with respect to the repeating units of GC. To study the aggregation-modulated ESIPT behavior of the HBO pendant, a model compound (GA–HBO) was prepared via the same amidation procedure with HBO-COOH and glucosamine to represent the substituted repeating unit of GC–HBO.

In the low-molecular-weight model study, the GA–HBO aggregates were prepared by a nanoprecipitation method in a water/THF mixed solvent where THF and water are good and poor solvents for the HBO unit, respectively. The degree of chromophoric aggregation was controlled at a constant concentration (10 μM) by changing water fraction (=water/[water + THF] × 100 by volume) of the mixed solvent. As shown in Fig. 2a, there exist two π–π* absorption bands at 333 and 345 nm in THF solution (0% water fraction) which can be assigned to the ground-state *syn*- and *anti*-rotational isomers of the enol tautomer, according to the reported assignments for the parent HBO molecule [18,19]. The feature of the solution absorption manifested no change up to 60% water fraction, indicating that GA–HBO kept being dissolved in a water-rich mixed solvent owing to the enhanced hydrophilicity by glucosamine substitution. From 80% water fraction upward, however, the main band at 320–360 nm became structureless along with hypsochromic and hypochromic effects as well as a remarkable baseline lift by Mie scattering. This spectral change is a typical indication for the formation of nanoaggregates, as evidenced by the particulate size distribution of the 100% water fraction sample (Fig. 2b): 37.3 ± 4.5 nm by dynamic light scattering (DLS) and 26.9 ± 7.1 nm by transmission electron microscopy (TEM). The suspension of self-aggregated GA–HBO nanoparticles exhibited fairly high colloidal stability, which is most likely attributed to the amphiphilicity by the water-soluble glucosamine substitution.

The fluorescence spectra of the ESIPT-active GA–HBO in solution and nanoaggregate dispersion are shown in Fig. 2c. In the monomer state in THF solution, the spectrum shows tautomeric dual emission bands with comparable intensity: a multi-peak band in the region of 400–450 nm and a broad one centered at 520 nm. ESIPT is a phototautomerization occurring in the excited state of intramolecularly hydrogen (H)-bonded molecules that exist in the enol (E) form in the ground state. Upon photoexcitation, the excited E form undergoes fast tautomerization to the excited keto (K) form through the intramolecular proton transfer, to generate the K emission that is far red-shifted compared to the normal E fluorescence. Therefore, the shorter- and the longer-wavelength bands of the solution spectrum in Fig. 2c can be assigned to the emission of rotational E isomers and the typical proton-transferred K emission with an abnormally large Stokes' shift, respectively. In the aggregated state, however, the spectrum is composed mainly of an intense K band peaking at 500 nm, along with a negligible component of the E emission below 450 nm. It is known that the intensity ratio between E/K emission

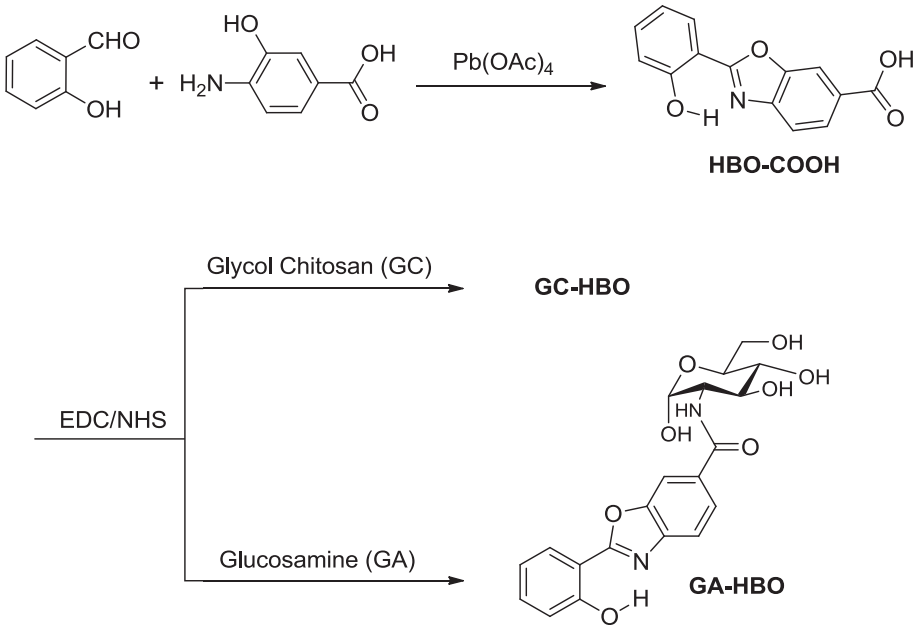

Scheme 1. Synthetic route of HBO-conjugated bio-amphiphiles.

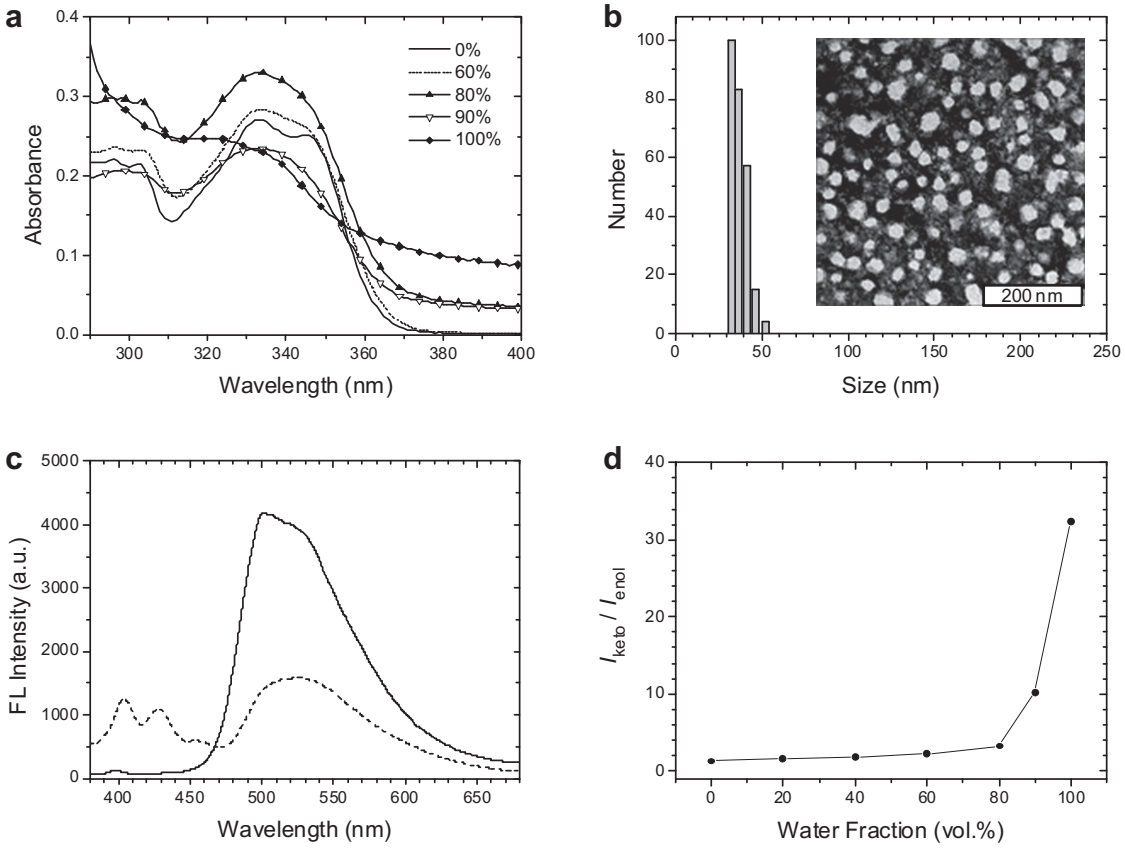

Fig. 2. Optical and morphological characteristics of GA–HBO in mixed solvents with varying water fraction (=water/[water + THF] × 100 by volume). (a) Absorption spectra of GA–HBO. Water fraction is indicated. (b) Number-averaged hydrodynamic size (measured by DLS) and TEM image (inset) of nanoaggregates formed in 100% water fraction. (c) Fluorescence spectra of GA–HBO solution (dotted line, in THF) and nanoaggregates (solid line, in water). (d) Ratiometric plot of fluorescence intensities at 510 nm (keto) and 400 nm (enol), as a function of water fraction.

bands of HBO is dependent on the molecular state: HBO emits strong E fluorescence with a weak K component when dissolved in H-bond perturbing solvents [18,19], whereas their K fluorescence can be greatly enhanced over the E emission in the aggregated state because the solidification prefers the energetically favored H-bonded geometry that is prerequisite for the ESIPT reaction [19]. In this context, the exclusive K emission from the GA–HBO nanoaggregates suggests that the HBO units in the solidified state exist dominantly in the *syn*-E conformation, where the phenyl hydroxyl proton forms an internal H bond with the benzoxazole nitrogen atom, to maximize the ESIPT efficiency [19,20]. Importantly, it was found that the intensity ratio between K and E emission bands (I_{keto}/I_{enol}) is modulated depending on the degree of aggregation (Fig. 2d), proving the utility of the ESIPT dual emission for the ratiometric fluorescence probing of aggregation-related molecular events.

The aggregation-probing potential of ESIPT dual fluorescence in an actual biopolymeric amphiphile system was evaluated with the self-assembly and ratiometric optical modulation behaviors of GC–HBO. It was found that the lyophilized GC–HBO solid after purification by dialysis forms a clear dispersion in water by sonication. Fig. 3a shows representative fluorescence spectra of the GC–HBO dispersion at a high concentration of 1 kg m^{-3}, the spectrum shows tautomeric dual bands. As discussed above in the model study, they can be assigned as E (400 nm) and K (~500 nm) emission of the HBO pendant. On considering the predominant K emission observed from the GA–HBO nanoaggregates (Fig. 2c), the E/K dual fluorescence from the GC–HBO dispersion indicates that the chemically conjugated hydrophobic pendants are not fully aggregated in water due to the interfering motion of the water-soluble backbone. With lowering concentration, the intensity of K emission was diminished significantly, while the E component was intensified. A plot of the intensity ratio between K and E components (I_{keto}/I_{enol}) versus the log of concentration shows a two-phase relationship, suggesting formation of self-assembled nanoparticles at higher concentrations (Fig. 3b). The observed inflection point (a crossing of the two linear fits in the plot) corresponds to a critical particulation concentration (CPC) of 0.04 kg m^{-3}, above which GC–HBO forms and retains the self-assembled nanostructure via chromophoric aggregation. The steady increase in I_{keto}/I_{enol} with increasing concentration below the CPC indicates gradual buildup of chromophoric aggregation toward self-assembly into particulate nanostructure.

TEM and DLS data in Fig. 3c directly evidence the formation of self-assembled GC–HBO nanoparticles above the CPC. The number-weighted hydrodynamic size distribution of a wet sample was determined as 87.1 ± 1.4 nm by DLS. The TEM image manifests that the dried GC–HBO nanoparticles are polydisperse in size with a shrunken diameter of 19.9 ± 11.1 nm (the inset of Fig. 3c). The size difference between the wet and dried samples suggests that the dispersed nanoparticles exist in the swollen state and shrink during the drying process. Below the CPC, no detectable scattering was observed in the detection limit of the DLS instrument, indicative of the disintegration of nanostructure. These results indicate that the chemical conjugation of HBO pendants efficiently introduces the hydrophobic and chromophoric π–π interactions to the free motion of the water-soluble GC backbone in aqueous environment,

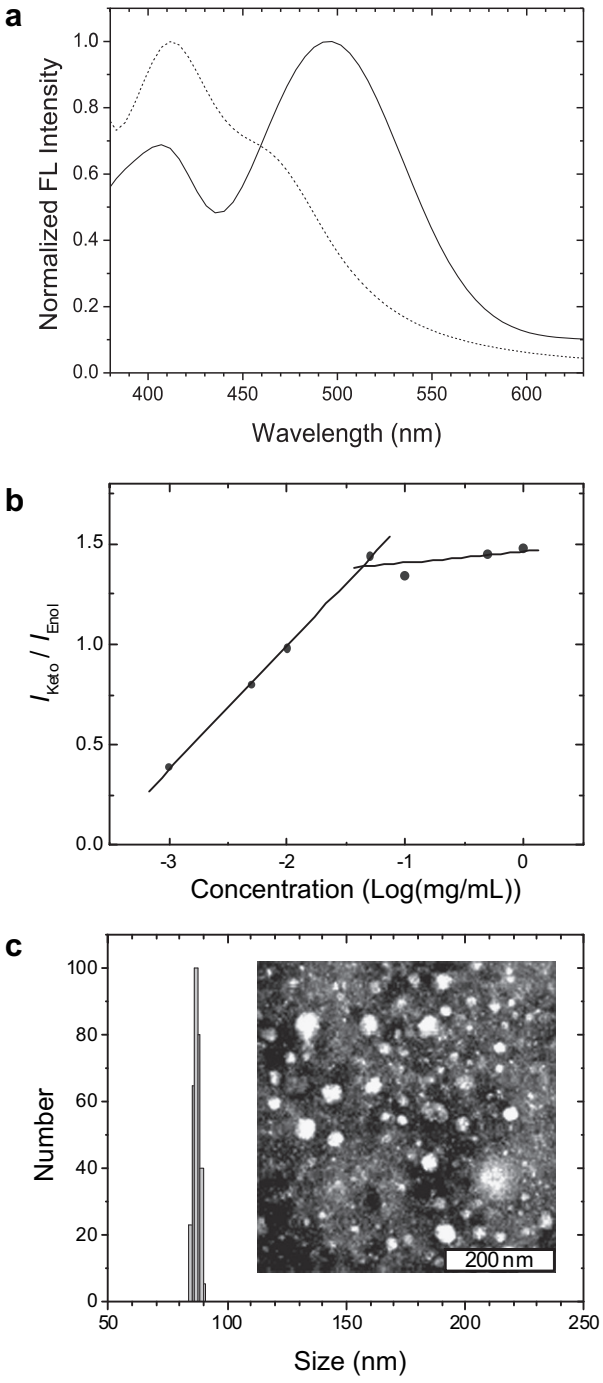

Fig. 3. Optical and morphological characteristics of GC–HBO in water with varying the amphiphilic polymer concentration. (a) Normalized fluorescence spectra at 1.0 kg m^{-3} (solid line) and 0.001 kg m^{-3} (dotted line). (b) Ratiometric plot of fluorescence intensities at 510 nm (keto) and 400 nm (enol), as a function of the log of concentration. The solid lines are the linear fits for experimental data in 0.001–0.05 kg m^{-3} and 0.05–1.0 kg m^{-3}, respectively. (c) Number-averaged hydrodynamic size (measured by DLS) and TEM image (inset) of self-assembled nanoparticles at 1.0 kg m^{-3}.

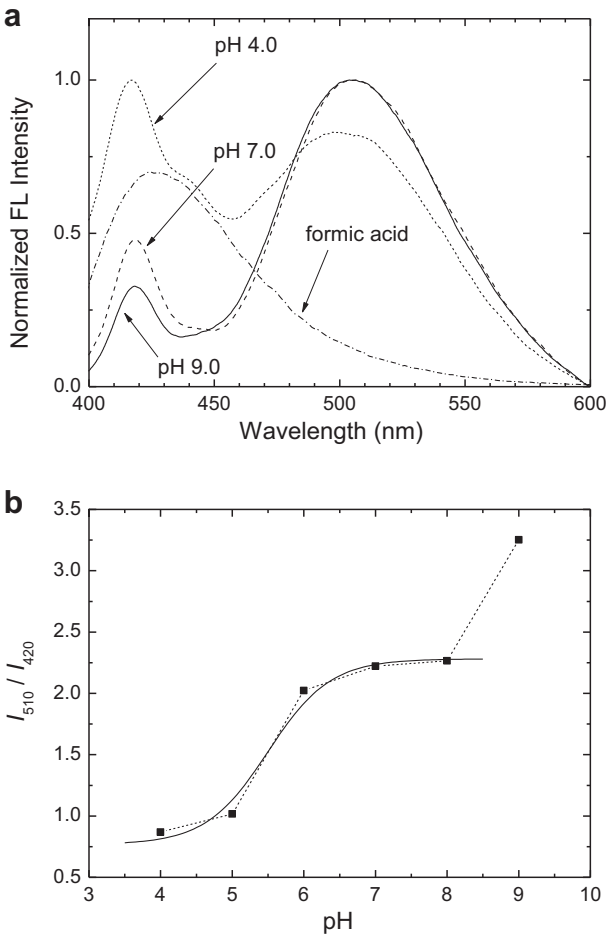

Fig. 4. pH response of GC–HBO dual emission. (a) Normalized fluorescence spectra in PBS with varying pH and formic acid. (b) Ratiometric plot of fluorescence intensities at 510 nm (keto) and 420 nm (enol and protonated enol), as a function of pH. The solid curve is the fitting result obtained by using Eqn. (1).

to induce the amphiphilic self-assembly into swollen nanoparticles. The concentration-dependence of I_{keto}/I_{enol} provides information on the concentration and self-assembly status of GC–HBO itself, to make it useful as a self-probing imaging agent.

In addition to the concentration-probing capability, the dual emission of GC–HBO nanoparticles exhibit pH-responsive spectral evolution, as observed in Fig. 4. When examined in phosphate buffer saline (PBS, pH 4.0–9.0), the K emission is the most dominant over the E component at the highest pH (pH 9.0) and the ratio (I_{keto}/I_{enol}) drops gradually with decreasing pH. This optical pH response is attributable to the basicity of GC–HBO arising from its chemical structure. As shown in Fig. 2, GC–HBO is composed of two basic constituents, i.e., unsubstituted repeating units of the GC backbone and benzoxazoles in the pendant. On the basis of the reported pK_a values of the protonated GC (pK_a ~ 6.5) [15] and the protonated HBO (pK_a ~ 1.3) [26], it is anticipated that protonation takes place at free amines in the GC backbone near neutral pH and then occurs at the benzoxazole nitrogen at lower pH. Partial protonation of the GC backbone at neutral pH may raise the hydrophilicity of amphiphilic GC–HBO and thus cause its formation of hydrogel-like swollen nanostructure in water, as discussed in Fig. 3c. The enhanced K emission at pH 9.0 (Fig. 4a) suggests that the GC backbone changes from the partially protonated state at neutral pH into a deprotonated free amine form by basification, which makes GC–HBO less hydrophilic to promote chromophoric aggregation of the ESIPT pendants via hydrophobically shifted amphiphilic balance. In this context, the opposite modulation of the dual emission at pH 4.0–5.0, i.e., intensified E emission over the K band, indicates that the degree of pendant aggregation, preferring the generation of K emission, is reduced at lower pH. One can expect that the hydrophilicity of GC–HBO will be maximized under the given acidic condition via dual protonation of the whole backbone and part of the HBO pendants. The occurrence of partial protonation at the pendants at lower pH is evidenced by the fluorescence spectrum

obtained at pH 4.0. As shown in Fig. 4a, the E emission band at pH 4.0 has a longer-wavelength shoulder that is well matched with the fully protonated emission from a GC–HBO solution in formic acid. It is noted that protonation of the benzoxazole amine interferes the internal H bond and thus blocks a pathway for ESIPT, to generate protonated enol fluorescence at the cost of phototautomeric (keto–enol) dual emission [5]. Accordingly, it is concluded that the partial pendant protonation decreases the K/E emission ratio of GC–HBO by disturbing the chromophoric aggregation as well as by intensifying the E emission range due to the spectral similarity between E and protonated bands. The obtained titration plot of I_{keto}/I_{enol} enables ratiometric pH probing in the range of pH 4–8 (Fig. 4b). This result suggests that the pendant protonation-assisted hydrophilicity enhancement of GC–HBO and the cooperative dual emission modulation thereby lead to the nanoscopically improved pH sensitivity in spite of a low pK_a value of the pendant unit [23]. From the nonlinear fitting of the pH response (the solid line in Fig. 4b), the resulting pK_a value (determined by the overall self-assembly behavior of GC–HBO) was extracted as ~5.1, which is useful for pH measurement in the cell's acidic organelles such as endosomes or lysosomes [27].

4. Conclusions

We have designed and prepared a new biopolymeric hybrid (GC–HBO) that is composed of a hydrophilic GC backbone and densely conjugated hydrophobic ESIPT pendants, to take advantage of the resulting correlation between the amphiphilic assembly behavior and the dual emission modulation thereby. It has been demonstrated that GC–HBO can self-assemble into nanoparticles in aqueous phase by chromophoric aggregation and generate signal modulation of dual emission responsive to the changes in self-concentration and surrounding pH. We anticipate that the ratiometric fluorescence response of GC–HBO will offer a possible way to study the molecular aggregation behavior of self-assembled biopolymeric nanoparticles in an in vivo system with complex biodistribution and varying pH.

Acknowledgment

This work was supported by the Real-Time Molecular Imaging Project and the Pioneer Research Program (2009-0081523) funded by the Korea Ministry of Education, Science and Technology (MEST). The work at Seoul National University was supported by the Basic Science Research Program through the National Research Foundation of Korea (NRF) funded by MEST (CRI; RIAMIAM0209 (0417-20090011)).

References

[1] Krämer R. Fluorescent chemosensors for Cu^{2+} ions: fast, selective, and highly sensitive. Angewante Chemie International Edition 1998;37:772–3.
[2] Strehmel B. Fluorescence probes for material science. In: Nalwa HS, editor. Advanced functional molecules and polymers, vol. 3. Gordon and Breach Science Publishers 2001. p. 299.
[3] de Silva AP, McClenaghan ND. Simultaneously multiply-configurable or superposed molecular logic systems composed of ICT (internal charge transfer) chromophores and fluorophores integrated with one- or two-ion receptors. Chemistry-A European Journal 2002;8:4935–45.
[4] Lakowicz JR, Malicka J, Gryczynski I, Gryczynski Z, Geddes CDJ. Radiative decay engineering: the role of photonic mode density in biotechnology. Journal of Physics D: Applied Physics 2003;36:R240–9.
[5] Kim S, Park SY. Photochemically gated protonation effected by intramolecular hydrogen bonding: towards stable fluorescence imaging in polymer films. Advanced Materials 2003;15:1341–4.
[6] Luo J, Xie Z, Lam JWY, Cheng L, Chen H, Qiu C, et al. Aggregation-induced emission of 1-methyl-1,2,3,4,5-pentaphenylsilole. Chemical Communications 2001:1740–1.
[7] An B-K, Kwon S-K, Jung S-D, Park SY. Enhanced emission and its switching in fluorescent organic nanoparticles. Journal of the American Chemical Society 2002;124:14410–5.
[8] Xiao D, Xi L, Yang W, Fu H, Shuai Z, Fang Y, et al. Size-tunable emission from 1,3-diphenyl-5-(2-anthryl)-2-pyrazoline nanoparticles. Journal of the American Chemical Society 2003;125:6740–5.
[9] Ryu SY, Kim S, Seo J, Kim Y-W, Kwon O-H, Jang D-J, et al. Strong fluorescence emission induced by supramolecular assembly and gelation: luminescent organogel from nonemissive oxadiazole-based benzene-1,3,5-tricarboxamide gelator. Chemical Communications 2004:70–1.
[10] Kim S, Zheng Q, He GS, Bharali DJ, Pudavar HE, Baev A, et al. Aggregation-enhanced fluorescence and two-photon absorption in nanoaggregates of a 9,10-bis[4′-(4″-aminostyryl)styryl]anthracene derivative. Advanced Functional Materials 2006;16:2317–23.
[11] Lim C-K, Kim S, Kwon IC, Ahn C-H, Park SY. Dye-condensed biopolymeric hybrids: chromophoric aggregation and self-assembly toward fluorescent bionanoparticles for near infrared bioimaging. Chemistry of Materials 2009; 21:5819–25.
[12] Lee KY, Kwon IC, Kim Y-H, Jo WH, Jeong SY. Preparation of chitosan self-aggregates as a gene delivery system. Journal of Controlled Release 1998;51:213–20.
[13] Kim K, Kwon S, Park JH, Chung H, Jeong SY, Kwon IC. Characterizations of size-controlled self-aggregates based on glycol chitosans modified with deoxycholic acid. Biomacromolecules 2005;6:1154–8.
[14] Park K, Kim J-H, Nam YS, Lee S, Nam HY, Kim K, et al. Effect of polymer molecular weight on the tumor targeting characteristics of self-assembled glycol chitosan nanoparticles. Journal of Controlled Release 2007;122:305–14.
[15] Nam HY, Kwon SM, Chung H, Lee S-Y, Kwon S-H, Jeon H, et al. Cellular uptake mechanism and intracellular fate of hydrophobically modified glycol chitosan nanoparticles. Journal of Controlled Release 2009;135:259–67.
[16] Krishnamurthy M, Dogra SK. Proton transfer of 2-(2′-hydroxyphenyl)benzoxazole in the excited singlet state. Journal of Photochemistry 1986;32:235–42.
[17] Elsaesser T, Schmetzer B. Excited-state proton transfer in 2-(2'-hydroxyphenyl)benzothiazole: formation of the anion in polar solvents. Chemical Physics Letters 1987;140:293–9.
[18] Abou-Zied OK, Jimenezm R, Thompson EHZ, Millar DP, Romseberg FE. Solvent-dependent photoinduced tautomerization of 2-(2′-hydroxyphenyl) benzoxazole. The Journal of Physical Chemistry A 2002;106:3665–72.
[19] Huang J, Peng A, Fu H, Ma Y, Zhai T, Yao J. Temperature-dependent ratiometric fluorescence from an organic aggregates system. The Journal of Physical Chemistry A 2006;110:9079–83.
[20] Chang DW, Kim S, Park SY. Excited-state intramolecular proton transfer via a preexisting hydrogen bond in semirigid polyquinoline. Macromolecules 2000;33:7223–5.
[21] Kim S, Seo J, Park SY. Torsion-induced fluorescence quenching in excited-state intramolecular proton transfer (ESIPT) dyes. Journal of Photochemistry and Photobiology A: Chemistry 2007;191:19–24.
[22] Kim H-J, Lee J, Kim T-H, Lee TS, Kim J. Highly emissive self-assembled organic nanoparticles having dual color capacity for targeted immunofluorescence labeling. Advanced Materials 2008;20:1117–21.
[23] Kim S, Pudavar HE, Prasad PN. Dye-concentrated organically modified silica nanoparticles as a ratiometric fluorescent pH probe by one- and two-photon excitation. Chemical Communications; 2006:2071–3.
[24] Charier S, Ruel Odile, Baudin J-B, Alcor Damien, Allemand J-F, Meglio A, et al. An efficient fluorescent probe for ratiometric pH measurements in aqueous solutions. Angewante Chemie International Edition 2004;43:4785–8.
[25] Kim S, Sohn J, Park SY. Synthesis and phase behavior of chiral liquid crystalline monomers and polymers containing 2-phenylbenzoxazole moiety in mesogenic unit. Bulletin of the Korean Chemical Society 1999;20:473–7.
[26] Mordziński A, Grabowska A. Intramolecular proton transfer in excited benzoxazoles. Chemical Physics Letters 1982;90:122.
[27] Haugland RP. Handbook of fluorescent probes and research products. 9th ed. Eugene: Molecular Probes Inc; 2002.